V.M. Kryshenik[1], A.I. Pogodin[2], M.J. Filep[2,3], I.M. Voynarovych[1], M.M. Pop[2], V.V. Rubish[1], A.V. Gomonnai[1]

Optical properties of As$_2$S$_3$:Ag glasses

[1]*Institute of Electron Physics, Nat. Acad. Sci. Ukr., Uzhhorod, Ukraine, kryshenik@gmail.com*
[2]*Uzhhorod National University, Uzhhorod, Ukraine*
[3]*Ferenc Rákóczi II Transcarpathian Hungarian Institute, Berehovo, Ukraine*

The paper describes the results of the studies of the effect of silver incorporation degree in newly synthesised Ag$_x$(As$_2$S$_3$)$_{1-x}$ ($0 \leq x \leq 0.2$) glasses on their optical absorption edge, bandgap energy, and refractive index dispersion in the visible and near-infrared range. The obtained experimental dependences are analysed using a single-oscillator Wemple–DiDomenico model. The optical bandgap energy as well as the single oscillator energy is shown to decrease with the Ag content in the glass while the dispersion energy increases and the bond ionicity degree remains practically unchanged.

Keywords: amorphous chalcogenides, superionic glasses, absorption edge, refractive index.

Introduction

Intense studies of chalcogenide glasses (ChG) in the recent decades provided a considerable array of data on their unique structural, electric, and optical properties [1–3]. In general, chalcogenide materials are distinguished by their high ability of glass-forming and a possibility of the chemical composition to be widely varied, capability of doping by transition metals, the amorphous state being completely preserved [4]. ChG are transparent in the infrared range, sensitive to illumination by light, they demonstrate a variety of photostructural effects, possess high refractive index and reasonable chemical and mechanical stability [1, 3]. This enables the application of ChG in all-optical switching and optical waveguides) [5–10]; in particular, they are suitable for the fabrication of on-chip chalcogenide microresonators with low-threshold parametric oscillation [11] and glass microfibers for mid-infrared optics [12]. ChG can be employed in multiphoton lithography for the formation of microstructures [13], as base materials for chalcogenide-based near-infrared photonic crystals [14–16], etc. Due to their good thermoelectric properties ChG are considered promising objects of study to implement a new generation of solid-state cooling systems and thermoelectric generators [17]. An ever increasing attention is paid to phase-change ChG, suitable for the production of memristive devices with the intention of being used for the means of data processing and storage, in particular, artificial neural networks [18, 19].

As–S ChG with silver atoms incorporated in their structure look attractive for researchers due to the dominating ionic type of conductivity and effective diffusion of Ag atoms; polarity-dependent electric switching with memory effect facilitates the fabrication of efficient non-volatile devices [20, 21]. An essential level of polarisability of chalcogen atoms compared to oxygen, their noticeable mobility as charged ions and in combination with Ag or Cu dopants made ChG an interesting class of objects for fundamental studies aiming at applications in solid-state ionics [22, 23].

Introduction of silver in the ChG of the As–S system, as well as the choice of technology for their fabrication, essentially affects their physical and chemical properties, for instance, charge-carrier mobility, value and type of electric conductivity, optical and thermoelectric properties, photosensitivity, etc. Doping with Ag (by several at. per cent) is capable of increasing the ionic conductivity by at least five orders of magnitude and

strongly affects physical and chemical properties of the material. Dramatic changes of such kind in the ionic transport are inevitably related to the structural arrangement of the glasses.

In the recent years, ChG with noble metal nanoparticles incorporated in their structure attract an extended interest, especially in view of their possible application in memory switching devices [4, 22, 24] as well as in programmable metallization-cells in solid electrolytes [25].

Illumination of noble metal-doped chalcogenide glasses used as a base medium for photoionics, initiates migration of the incorporated metal atoms, leading to the modulation of reflection, transmission, and absorption of optical waves [21, 26, 27].

Note that earlier studies of glasses of the Ag–As–S system mostly concerned their basic characteristics along $(Ag_2S)–(As_2S_3)$ [28–34] and $Ag–AsS_2$ pseudo-binary lines [35–38].

The present paper is aimed at the studies of optical properties of synthesised $Ag_x(As_2S_3)_{1-x}$ glasses $(0 \leq x \leq 0.20)$. We took into account the fact that introduction of silver atoms in As_2S_3 affects the glass-forming ability of the system which for the $Ag_x(As_2S_3)_{1-x}$ glasses $(0 < x < 0.44)$ encompasses a rather broad compositional interval except a section with potential tendency toward crystallisation when Ag content is within 13 to 21 vol. % [39].

I. Experimental

Silver-doped $Ag_x(As_2S_3)_{1-x}$ glasses $(0 \leq x \leq 0.2)$ were obtained from pre-synthesised As_2S_3 glass and colloidal Ag particles by single-temperature synthesis in evacuated quartz ampoules at 600 ºC. At this maximal temperature the melt was kept at constant stirring for 4 h and afterwards sharply quenched on air. The synthesis led to $Ag_x(As_2S_3)_{1-x}$ glasses with $x = 0.02, 0.04, 0.06, 0.08, 0.10, 0.15,$ and $0.2,$ the colour of which was varied from light yellow to dark red with increasing Ag content.

Binary As_2S_3 glass was synthesised from elemental components (99.999% purity) in the stoichiometric composition in a quartz ampoule evacuated to 10^{-2} Pa, constantly rotating around its axis. The ampoule was heated to 920 K. The mass of the mixture loaded in the ampoule typically was 9–12 g.

Colloidal silver in the form of nanoparticles was obtained by reduction of AgCl by hydrazine chloride $(N_2H_6Cl_2)$ in an alkaline medium (NaOH). AgNO₃ and KCl were used to obtain AgCl. Purity of $AgNO_3$, KCl, $N_2H_6Cl_2$, and NaOH was not worse than 99.95%. Note that the concentration of the salt solutions prepared in doubly distilled water was 1 mole/l. The reduction process was carried out at 80 ºC.

XRD studies were performed using a Proto Manufacturing Ltd diffractometer equipped with a DECTRIS MYTHEN2R 1D hybrid photon detector. The measurements were carried out in the Bragg-Brentano geometry using a Cu K_α X-ray source.

Optical transmission measurements for the As_2S_3:Ag glasses were carried out in the range 400–1100 nm using a Shimadzu UV-1700 spectrophotometer. Refraction

index dispersion of the As_2S_3:Ag glasses was studied in the spectral range 440–1000 nm using a Horiba Smart SE spectral ellipsometer. During the measurements the optical beam was incident on the studied sample at an angle of 70°. The obtained experimental spectra were analysed using DeltaPsi2 software.

II. Results and Discussion

X-ray diffractograms for the As_2S_3:Ag of various compositions are reproduced in Fig. 1. They demonstrate broad smooth maxima, typical for amorphous media, not much differing from the XRD pattern of the binary As_2S_3 glass. There is no evidence for possible crystalline inclusions in the samples under investigation. This result is even more interesting for the glasses with Ag content of 15 and 20 molar %, since in earlier studies [39, 40] these ternary compositions, according to the phase diagram presented, are considered not prone to glass-forming (Fig. 2).
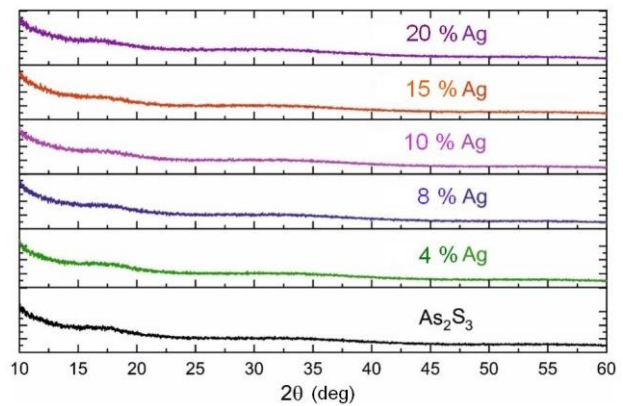

Fig. 1. X-ray diffractograms for undoped and silver-doped samples of As_2S_3 glass.
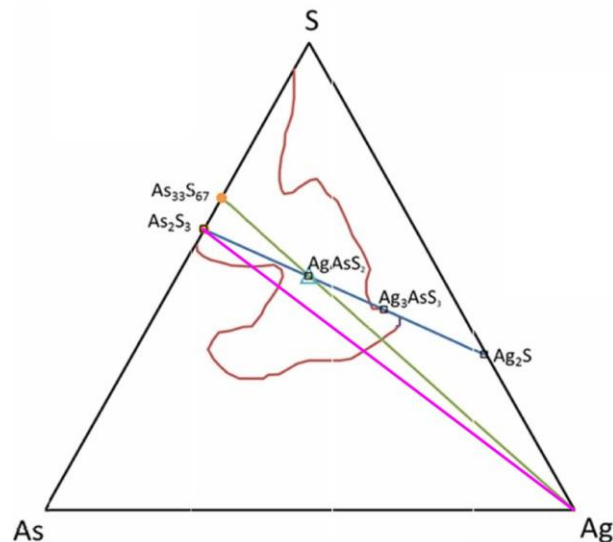

Fig. 2. Glass-forming region in Ag–As–S ternary system, encompassed by the red line (adapted from Ref. [39]).

Note that silver, introduced into the glass structure, in this case is rather a structural network modifier of the chalcogenide glass than a network former [41]. In other words, when the silver concentration exceeds a

percolation limit, detected in multiple experiments (3–7 at. % Ag), this causes internal phase separation of the ChG in two phases – Ag-deficient and Ag-enriched [27, 30, 37, 38]. Differential scanning calorimetry showed this separation to result in the presence (on the macroscopic level) of two glass-forming temperatures: a lower one T_{g1} for the superionic (silver-enriched) phase and a higher one T_{g2} for the silver-deficient semiconductor phase [30]. Spinodal phase separation of such kind imposes certain restrictions on the possibility of further crystallisation transformations in the glass [42].

It is logical to assume that a great number of structural units in the ChG would noticeably affect their properties, namely optical bandgap, rigidity of the amorphous material structure, and the above-mentioned glass-forming temperature.

Simultaneously, we assume that the technology of glass synthesis employed here when silver was introduced in the synthesised glass structure by means of colloidal nanoparticles, can facilitate the phase separation and, accordingly, the extension of the glass-forming region in As₂S₃:Ag.

We take into account that in $Ag_x(As_2S_3)_{1-x}$ glasses introduction of silver leads to both compositional and topological disordering of the structure. As a result, density of localised states in the bandgap increases, directly affecting the shape of the low-energy tail of the optical absorption (Fig. 3).
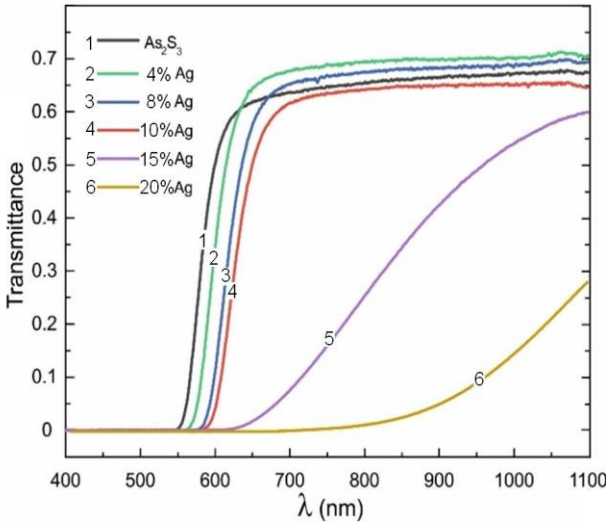

Fig. 3. Optical transmission spectra for $Ag_x(As_2S_3)_{1-x}$ glasses.

As can be seen from Fig. 4 and Fig. 5, with increasing silver concentration in $Ag_y(As_2S_3)_{1-y}$ the optical absorption edge shifts towards longer wavelengths and becomes less steep and noticeably smeared, with a deviation from the exponential shape.

The optical bandgap of the glasses E_g^* was calculated using the Tauc equation [43].

$$\alpha \cdot hv = B \cdot (hv - E_g^*)^2 \qquad (1)$$

where α is the optical absorption coefficient, hv is the photon energy, B is a ChG material-related parameter.
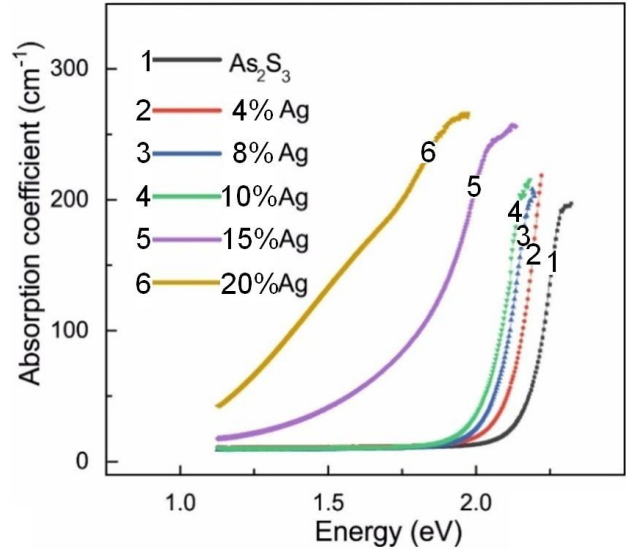

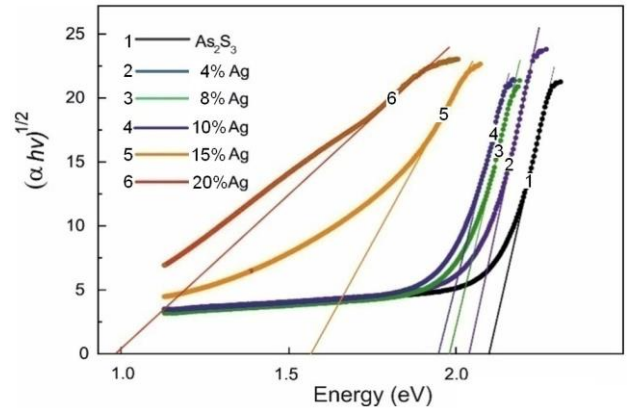**Fig. 4.** Optical absorption spectra for $Ag_x(As_2S_3)_{1-x}$ glasses.

Fig. 5. Dependences of the $(\alpha \cdot hv)^{1/2}$ parameter on the photon energy hv in $Ag_x(As_2S_3)_{1-x}$ glasses.

Whenever the silver content in the $Ag_x(As_2S_3)_{1-x}$ glasses exceeded 10 mol. %, we observed a nonlinear E_g^* decrease (Fig. 6). Such behaviour can be explained not only by the effect of structural and compositional types of disordering [33]. We assume that evident separation of microphases in the ternary As–Ag–S system occurs already at the stage of the glass synthesis and is determined by the effect of liquid-liquid non-mixing. As follows from the structural studies of glasses of the Ag–As–S system [27, 44], introduction of a relatively large amount of silver results not only in fragmentation of regions of the Ag-deficient phase, but also in an essential increase of number and active expansion of separate Ag-enriched regions. With increasing silver content, the latter comprise an ever increasing part of the glass volume, the size of each regions being hundreds of nanometers.

While calculating the behaviour of the refractive index of the As₂S₃:Ag glasses we used the Tauc–Lorentz model, in the framework of which an "air-glass-roughness" system was considered. For the glasses under investigation, in order to take into account the silver doping level, we used a system with a double base layer (Tauc–Lorentz model / Tauc–Lorentz+Drude model). The model employed is convenient for the ellipsometric studies of glasses to describe the refractive index

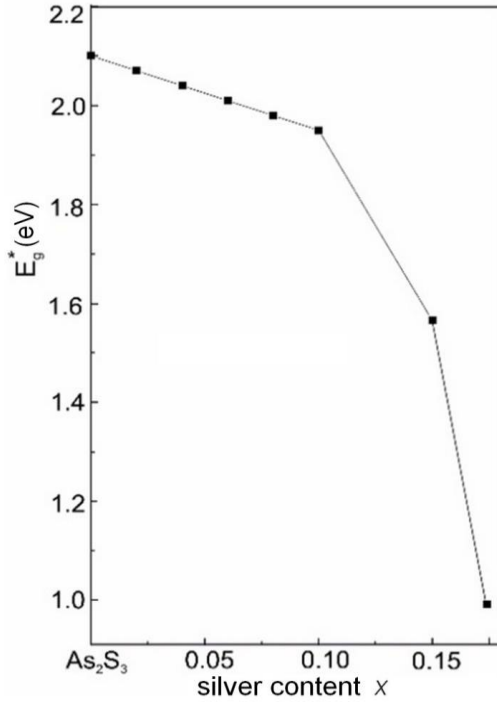dispersion $n(\lambda)$ close to the optical absorption edge.

Fig. 6. Dependence of the optical bandgap E_g^* on the Ag content in $Ag_x(As_2S_3)_{1-x}$ glasses.

Results of the ellipsometric studies of the refractive index dispersion $n(\lambda)$ for the As_2S_3:Ag glasses and dependence of this parameter at a fixed wavelength $\lambda=1$ μm on the silver content are reproduced in Fig. 7 and Fig. 8. The strong dispersion dependence $n(\lambda)$ revealed in the short-wavelength part of the spectrum (Fig. 7) is related to the vicinity of the fundamental absorption edge, while the observed shift of the dispersion curves correlates with the E_g^* variation versus the glass composition. With increasing Ag content a nonlinear increase of the refractive index was observed. A higher doping level led to a general refractive index increase due to an increasing glass density caused by the presence of ever increasing concentration of the Ag-enriched phase entities.
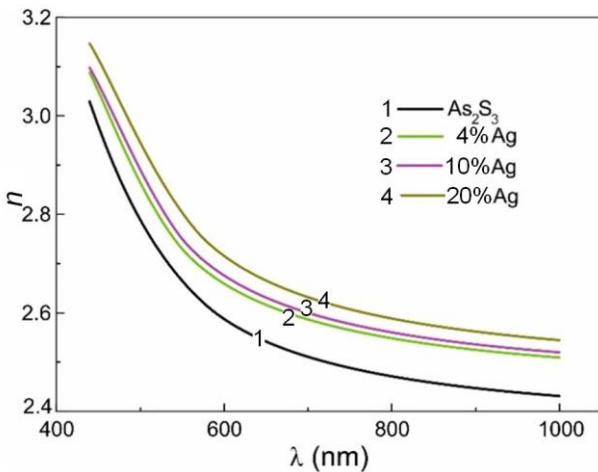

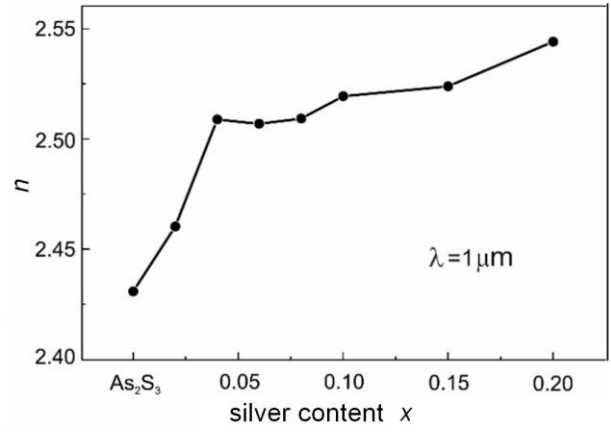**Fig. 7.** Refractive index dispersion $n(\lambda)$ in $Ag_x(As_2S_3)_{1-x}$ glasses.

Fig. 8. Dependence of the refractive index at a wavelength $\lambda=1$ μm on the content of Ag in $Ag_x(As_2S_3)_{1-x}$ glasses.

In order to analyse the spectral dependence of the refractive index n in the As_2S_3:Ag glasses, we applied a known single-oscillator model by Wemple–DiDomenico [45]. It is based on an equation which determines the relationship between the optical parameters of the glass:

$$n^2(E) - 1 = \frac{E_d^{WD} E_0^{WD}}{(E_0^{WD})^2 - (h\nu)^2} \tag{2}$$

where E_0^{WD} is the energy of intrinsic vibrations of the electron oscillator and E_d^{WD} is the dispersion energy, dependent of the material structure and chemical composition. The E_0^{WD} parameter approximately corresponds to the maximum of the imaginary part of the dielectric permittivity, hence it can be related to the average energy of transitions of electrons from the valence band to the conduction band. The dispersion energy E_d^{WD} relates cation coordination number N_c, anion valence Z_a and number of effective valence electrons N_v, bound to the anion:

$$E_d^{WD} = b \cdot N_c \cdot N_v \cdot Z_a \tag{3}$$

where b is a parameter, dependent of the bond degree of ionicity. It is known that for mostly ionic compounds $b = (0.26 \pm 0.04)$ eV and for covalent compounds $b = (0.37 \pm 0.04)$ eV [46]. The Z_a parameter characterises the polarisation degree, i. e. the effect of low-energy photons on the electron system, related to anions [46]. Introduction of silver in the As_2S_3 glass would be expected to increase the N_c value which should result in an increase of the dispersion energy E_d^{WD}.

Equation (2) in general gives a correct decription of the refractive index n due to the relationhip of n and E_g^*. The equation is quite correct when the dispersion of n is studied at a not very high optical absorption level [47, 48].

Characteristic parameters calculated for the As_2S_3:Ag glasses based on the Wemple–DiDomenico model are listed in Table 1. It is shown that with increasing Ag content in the As_2S_3:Ag glass the single oscillator energy E_0^{WD} nonlinearly decreases. The dispersion energy E_d^{WD} in this case nonlinearly increases. This fact is in a good agreement with a noticeable increase of the cation coordination number N_c with the incorporation of Ag atoms in the As_2S_3 glass [49]. Simultaneously, an essential level of disorder of the glass structure at a higher Ag

content leads to a lower steepness of the $\alpha(h\nu)$ curves in the vicinity of the absorption edge (Fig. 4).

Having taken into account a simple relationship $E_0^{WD} \approx 1,9\, E_g^{WD}$ [49], we confirmed the trend of narrowing of the bandgap E_g^{WD} (Table 1) at increasing Ag content in the compounds under study. The decrease of the E_g^{WD} parameter appeared not so strong as the experimentally obtained shift of the absorption edge for the Ag$_x$(As$_2$S$_3$)$_{1-x}$ glasses at $x \geq 0.10$ (Fig. 6). We relate it to the character of their phase separation and the increasing concentration of silver-enriched phase inclusions.

According to the Wemple–DiDomenico model [45], the values of the static refractive index n_0^{WD} and degree of the bond ionicity f_i^{WD} for As$_2$S$_3$:Ag glasses can be estimated using the following equations:

$$n_0^{WD} = \left[1 + \frac{E_d^{WD}}{E_0^{WD}}\right]^{1/2} \tag{4}$$

$$f_i^{WD} = \left[\frac{E_0^{WD}}{E_d^{WD}}\right]^{1/2} \tag{5}$$

We found that the static refractive index n_0^{WD} in the As$_2$S$_3$:Ag glasses remains almost unchanged in the long-wavelength range. With increasing silver content, n_0^{WD} nonlinearly increases (Table 1), however, its value is usually lower than n determined by ellipsometry at a fixed wavelength $\lambda = 1$ μm (Fig. 8). The ionicity degree f_i^{WD} is practically constant in the whole compositional interval under study.

Table 1.

Parameters, determined in the framework of the Wemple–DiDomenico model for the Ag$_x$(As$_2$S$_3$)$_{1-x}$ glasses

Sample	E_0^{WD} (eV)	E_d^{WD} (eV)	E_g^{WD} (eV)	n_0^{WD}	f_i^{WD}
As$_2$S$_3$	3.99	16.58	2.100	2.27	0.49
2% Ag	3.94	16.65	2.074	2.29	0.49
4% Ag	3.89	16.76	2.047	2.304	0.48
6% Ag	3.87	16.88	2.037	2.316	0.48
8% Ag	3.86	17.05	2.031	2.33	0.48
10% Ag	3.85	17.17	1.925	2.34	0.47
15% Ag	3.84	17.26	1.92	2.34	0.47
20 % Ag	3.83	17.29	1.915	2.35	0.47

Conclusions

The paper presents the results of investigation of optical properties of Ag$_x$(As$_2$S$_3$)$_{1-x}$ glasses ($0 \leq x \leq 0.2$) prepared by single-temperature synthesis from As$_2$S$_3$ and colloidal silver particles. The amorphous structure of the as-prepared glasses was confirmed by XRD. Optical absorption spectra and refractive index dispersion of glasses with different content of silver were studied in the visible and near-infrared spectral range. The shape of the spectra in the vicinity of the optical absorption edge in general corresponds to the Urbach rule, the increasing amount of silver in the glasses leading to the absorption edge shift towards the long-wavelength range.

Refractive index dispersion in the As$_2$S$_3$:Ag glasses with different content of silver was studied using ellipsometry measurements. The results obtained were analysed in the framework of a single-oscillator Wemple–DiDomenico model. The oscillator energy and the average energy of electron transition from the valence band to the conduction band are calculated; these parameters decrease with increasing silver content in the glass while the dispersion energy (oscillator strength) increases. The detected deviations of the experimentally obtained compositional dependences of the optical bandgap and the refractive index at a fixed wavelength from the parameters calculated based on the Wemple–DiDomenico model are explained by the character of the microstructure of glasses with high silver content where silver-deficient and silver-enriched regions are present.

Kryshenik V.M. – Institute of Electron Physics, National Academy of Sciences of Ukraine, Ph. D. (Phys. & Math.), Researcher at Department of Materials for Functional Electronics;
Pogodin A.I. – Uzhhorod National University, Ph. D (Chem.), Senior Researcher;
Filep M.J. – Ferenc Rákóczi II Transcarpathian Hungarian Institute, Ph. D. (Chem.), Senior researcher, Associate Professor at Department of Biology and Chemistry;
Voynarovych I.M. – Institute of Electron Physics, National Academy of Sciences of Ukraine, Ph. D. (Phys. & Math.), Senior Researcher at Department of Materials for Functional Electronics;
Pop M.M. – Uzhhorod National University, Ph. D. (Phys. & Math.), Associate Professor at Department of Applied Physics;
Rubish V.V. – Institute of Electron Physics, National Academy of Sciences of Ukraine, Ph. D. (Phys. & Math.), Leading Engineer at Department of Quantum and Plasma Electronics;
Gomonnai A.V. – Institute of Electron Physics, National Academy of Sciences of Ukraine, Doctor of Sciences, Professor, Head of Department of Materials for Functional Electronics.

[1] K. Tanaka, K. Shimakawa. *Amorphous Chalcogenide Semiconductors and Related Materials* (Springer, 2021). https://doi.org/10.1007/978-3-030-69598-9.

[2] A. Zakery, S.R Elliott, *Optical properties and applications of chalcogenide glasses: a review,* J. Non-Cryst. Solids, 330, 1 (2003); https://doi.org/10.1016/j.jnoncrysol.2003.08.064.

[3] K. Shimakawa, A. Kolobov, S.R. Elliott, *Photoinduced effects and metastability in amorphous semiconductors and insulators,* Adv. Phys., 44(6), 475 (1995); https://doi.org/10.1080/00018739500101576.

[4] T. Wagner, B. Zhang, M. Fraenkl, S. Valkova, R. Vala, T. Hrbek, *Metal-doped chalcogenides.* In: The world scientific reference of amorphous materials: Structure, Properties, Modeling and Main Applications, Vol. 1 – Structure, Properties, Modeling and Applications of Amorphous Chalcogenides, A.V. Kolobov, K. Shimakawa (Eds.) (World Scientific 2021) 593–649. https://doi.org/10.1142/9789811215575_0018.

[5] B. J. Eggleton, B. Luther-Davies, K. Richardson, *Chalcogenide photonics.* Nat. Photonics, 5, 141 (2011); https://doi.org/10.1038/nphoton.2011.309.

[6] L. Li, H. Lin, S. Qiao, Y. Zou, S. Danto, K. Richardson, J. D. Musgraves, N. Lu, J. Hu, *Integrated flexible chalcogenide glass photonic devices,* Nat. Photonics, 8, 643 (2014); https://doi.org/10.1038/nphoton.2014.138.

[7] V.M. Kryshenik, Yu.M. Azhniuk, V.S. Kovtunenko, *All-optical patterning in azobenzene polymers and amorphous chalcogenides*, J. Non-Cryst. Solids, 512, 112 (2019); https://doi.org/10.1016/j.jnoncrysol.2019.02.019.

[8] B. Luther-Davies, *Integrated optics: flexible chalcogenide photonics,* Nat. Photonics, 8, 591 (2014); https://doi.org/10.1038/nphoton.2014.169.

[9] V. M. Kryshenik, *Dynamic photoinduced changes of optical characteristics and effect of optical memory in amorphous As–S film-based waveguides,* J. Non-Cryst. Solids, 585, 121528 (2022); https://doi.org/10.1016/j.jnoncrysol.2022.121528.

[10] P. Jean, A. Douaud, S. LaRochelle, Y. Messaddeq, W. Shi, *Silicon subwavelength grating waveguides with high-index chalcogenide glass cladding,* Opt. Express, 29(13), 20851 (2021); https://doi.org/10.1364/OE.430204.

[11] B. Zhang, P. Zeng, Z. Yang, D. Xia, J. Zhao, Y. Sun, Y. Huang, J. Song, J. Pan, H. Cheng, D. Choi, Z. Li, *On-chip chalcogenide microresonators with low-threshold parametric oscillation*, Photonics Res., 9(7), 1272 (2021); https://doi.org/10.1364/PRJ.422435.

[12] Y. Wang, S. Dai, *Mid-infrared supercontinuum generation in chalcogenide glass fibers: a brief review,* PhotoniX, 2(1), 9 (2021); https://doi.org/10.1186/s43074-021-00031-3.

[13] C.M. Schwarz, S.M. Kuebler, C. Rivero-Baleine, B. Triplett, M.Kang, Q. Altemose, C. Blanco, K.A. Richardson, Q. Du, S. Deckoff-Jones, J. Hu, Yifei Zhang, Y. Pan, C. Ríos, *Structurally and morphologically engineered chalcogenide materials for optical and photonic devices,* J. Opt. Microsyst., 1(1), 013502 (2021); https://doi.org/10.1117/1.JOM.1.1.013502.

[14] K.K. Suzuki, T. Baba, *Nonlinear light propagation in chalcogenide photonic crystal slow light waveguides,* Opt. Express, 18(25), 26675 (2010); https://doi.org/10.1364/OE.18.026675.

[15] L. Wei, J. Qian, L. Dong, M. Lu, *Chalcogenide photonic crystals fabricated by soft imprint-assisted photodoping of silver,* Small,16(19), 2000472 (2020); https://doi.org/10.1002/smll.202000472.

[16] I. Anghel, A. Petris, , *Design of an all-optical tunable 2D photonic crystal in As₂S₃ film*, Opt. Commun, 574, 131247 (2024); https://doi.org/10.1016/j.optcom.2024.131247.

[17] S. Y. Tee, D. Ponsford, C. L. Lay, X. Wang, X. Wang, D. C. J. Neo, T. Wu, Th Warintorn, J. C. C. Yeo, G. Guan, T.-C. Lee, M. Y. Han, *Thermoelectric silver-based chalcogenides,* Adv. Sci., 9(36), 2204624 (2022); https://doi.org/10.1002/advs.202204624.

[18] M. Wuttig, H. Bhaskaran, T. Taubner, *Phase-change materials for non-volatile photonic applications,* Nat. Photonics,11(8), 465 (2017); https://doi.org/10.1038/nphoton.2017.126.

[19] B. Gholipour, P. Bastock, C. Craig, K. Khan, D. Hewak, C. Soci, *Amorphous metal-sulphide microfibers enable photonic synapses for brain-like computing,* Adv. Opt. Mater., 3(5), 635 (2015); https://doi.org/10.1002/adom.201400472.

[20] S.G. Sarwat, T. Moraitis, C.D. Wright, H. Bhaskaran, *Chalcogenide optomemristors for multi-factor neuromorphic computation,* Nat. Commun., 13(1), 2247 (2022); https://doi.org/10.1038/s41467-022-29870-9.

[21] A.H. Elfarash, B. Gholipour, *Reconfigurable nanoionic and photoionic material and device platforms,* Adv. Phys., X 9(1), 2338285 (2024); https://doi.org/10.1080/23746149.2024.2338285.

[22] A. Pradel, M. Ribes, 7 – *Ionic conductivity of chalcogenide glasses*, In: J.-L. Adam, X. Zhang (Eds.), Chalcogenide Glasses, (Woodhead Publishing 2014) 169–208. https://doi.org/10.1533/9780857093561.1.169.

[23] B. Gholipour, S. R. Elliott, M. J. Müller, M. Wuttig, D. W. Hewak, B. E. Hayden et al., *Roadmap on chalcogenide photonics,* J. Phys. Photonics, 5(1), 012501 (2023); https://doi.org/10.1088/2515-7647/ac9a91.

[24] K.O. Čajko, D.L. Sekulić, S.R. Lukić-Petrović, *Dielectric and bipolar resistive switching properties of Ag doped As–S–Se chalcogenide for non-volatile memory applications,* Mater. Chem. Phys., 296, 127301 (2023); https://doi.org/10.1016/j.matchemphys.2023.127301.

[25] M. Mitkova, Y. Sakaguchi, D. Tenne, S. K. Bhagat, T.L. Alford, *Structural details of Ge–rich and silver–doped chalcogenide glasses for nanoionic nonvolatile memory*, Phys. Status Solidi A, 207(3), 621 (2010); https://doi.org/10.1002/pssa.200982902.

[26] Y. Murakami, M. Wakaki, S. Kawabata, *In-situ observation of photodoping phenomena in chalcogenide glass by spectroscopic ellipsometry,* Phys. Status Solidi C, 5(5), 1283 (2008); https://doi.org/10.1002/pssc.200777797.

[27] F. Kyriazis, A. Chrissanthopoulos, V. Dracopoulos, M. Krbal, T. Wagner, M. Frumar, S. N. Yannopoulos, *Effect of silver doping on the structure and phase separation of sulfur-rich As–S glasses: Raman and SEM studies*, J. Non-Cryst. Solids, 355(37-42), 2010 (2009); https://doi.org/10.1016/j.jnoncrysol.2009.04.070.

[28] M. Ohto, M. Itoh, K. Tanaka, *Optical and electrical properties of Ag–As–S glasses*, J. Appl. Phys., 77(3), 1034 (1995); https://doi.org/10.1063/1.359581.

[29] A. Piarristeguy, M. Ramonda, N. Kuwata, A. Pradel, M. Ribes, *Microstructure of Ag₂S–As₂S₃ glasses,* Solid State Ion. 177(35-36), 3157 (2006); https://doi.org/10.1016/j.ssi.2006.07.054.

[30] C. Holbrook, P. Chen, D. I. Novita, P. Boolchand, *Origin of conductivity threshold in the solid electrolyte glass system: $(Ag_2S)_x(As_2S_3)_{1-x}$*, IEEE Trans. Nanotechnol., 6(5), 530 (2007); https://doi.org/10.1109/TNANO.2007.905540.

[31] E. Bychkov, *Superionic and ion-conducting chalcogenide glasses: Transport regimes and structural features,* Solid State Ion., 180(6-8), 510 (2009); https://doi.org/10.1016/j.ssi.2008.09.013.

[32] I.I. Shpak, I. Studenyak, O. Shpak, *Temperature dependence of the refractive index of vitreous alloys of the Ag-As-S system,* Phys. Chem. Solid State, 19(3), 234 (2018); https://doi.org/10.15330/pcss.19.3.234-238.

[33] I.P. Studenyak, O.I. Shpak, M. Kranjčec, M.M. Pop, I.I. Shpak, P. Kisała, P. Panas, R. Romaniuk, U. Zhunissova, A. Ormanbekova, *Temperature studies of optical absorption edge in $(Ag_2S)_x(As_2S_3)_{1-x}$ (x<0.2) superionic glasses*, Proc. SPIE 11581, Photonics Applications in Astronomy, Communications, Industry, and High Energy Physics Experiments 2020, 115810T, 220 (2020); https://doi.org/10.1117/12.2580494.

[34] R. Zaiter, M. Kassem, D. Fontanari, M. Bokova, F. Cousin, T. Usuki, E. Bychkov, *Chemically-invariant percolation in silver thioarsenate glasses and two ion-transport regimes over 5 orders of magnitude in Ag content,* J. Non-Cryst. Solids, 584, 121513 (2022); https://doi.org/10.1016/j.jnoncrysol.2022.121513.

[35] M. Krbal, T.Wagner, T. Srba, J. Schwarz, J. Orava, T. Kohoutek, V. Zima, L. Benes, S. O. Kasap, M. Frumar, *Properties and structure of $Ag_x(As_{0.33}S_{0.67})_{100-x}$ bulk glasses,* J. Non-Cryst. Solids, 353(13-15), 1232 (2007); https://doi.org/10.1016/j.jnoncrysol.2006.11.024.

[36] S. Stehlik, J. Kolar, M. Bartos, M. Vlcek, M. Frumar, V. Zima, T. Wagner *Conductivity in Ag–As–S (Se, Te) chalcogenide glasses*, Solid State Ion., 181(37-38), 1625 (2010); https://doi.org/10.1016/j.ssi.2010.09.016.

[37] S. Stehlik, J. Kolar, H. Haneda, I. Sakaguchi, M. Frumar, T. Wagner, *Phase separation in chalcogenide glasses: the system AgAsSSe*, Int. J. Appl. Glass Sci., 2(4), 301 (2011); https://doi.org/10.1111/j.2041-1294.2011.00065.x.

[38] I. Kaban, P. Jóvári, T. Wágner, M. Bartoš, M. Frumar, B. Beuneu, W. Hoyer, N. Mattern, J. Eckert, *Structural study of AsS₂–Ag glasses over a wide concentration range,* J. Non-Cryst. Solids, 357(19-20), 3430 (2011); https://doi.org/10.1016/j.jnoncrysol.2011.06.015.

[39] T. Kawaguchi, *A structural study of Ag-rich Ag–As–S glasses,* Jpn. J. Appl. Phys., 37(1R), 29 (1998); https://doi.org/10.1143/JJAP.37.29.

[40] T. Kawaguchi, S. Maruno, S. R. Elliott, , *Compositional dependence of the photoinduced surface deposition of metallic silver in Ag–As–S glasses,* J. Non-Cryst. Solids, 211(1-2), 187 (1997); https://doi.org/10.1016/S0022-3093(96)00625-4.

[41] M. Mitkova, Y. Wang, P. Boolchand, *Dual chemical role of Ag as an additive in chalcogenide glasses,* Phys. Rev. Lett., 83(19), 3848 (1999); https://doi.org/10.1103/PhysRevLett.83.3848.

[42] A. Piarristeguy, R. Le Parc, M. Ramonda, R. Escalier, I. Grillo, G. J. Cuello, V. Cristiglio, A. Pradel, *Local vibrational and mechanical characterization of Ag conducting chalcogenide glasses,* J. Alloys Compd., 762, 906 (2018); https://doi.org/10.1016/j.jallcom.2018.05.280.

[43] J. Tauc, A. Menth, *States in the gap,* J. Non-Cryst. Solids, 8, 569 (1972); https://doi.org/10.1016/0022-3093(72)90194-9.

[44] A. Stronski, L. Revutska, A. Meshalkin, O. Paiuk, E. Achimova, A. Korchovyi, K. Shportko, O. Gudymenko, A. Prisakar, A. Gubanova, G. Triduh, *Structural properties of Ag–As–S chalcogenide glasses in phase separation region and their application in holographic grating recording,* Opt. Mater., 94, 393 (2019); https://doi.org/10.1016/j.optmat.2019.06.016.

[45] S. H. Wemple, M. DiDomenico *Behavior of the electronic dielectric constant in covalent and ionic materials* Jr, Phys. Rev., B 3(4), 1338 (1971); https://doi.org/10.1103/PhysRevB.3.1338.

[46] J. M. González-Leal, *The Wemple–DiDomenico model as a tool to probe the building blocks conforming a glass,* Phys. Status Solidi, B 250(5), 1044 (2013); https://doi.org/10.1002/pssb.201248487.

[47] O.I. Shpak, M.M. Pop, I.I. Shpak, I.P. Studenyak, *Refractometric studies of chalcogenide glasses in Ag–As–S system,* Opt. Mater., 35(2), 297 (2012); https://doi.org/10.1016/j.optmat.2012.09.004.

[48] S.I. Vyatkin, O.N. Romanyuk, S.V. Pavlov, A. Kotyra, A. Mussabekova, *Offsetting and blending with perturbation functions*, Proc. SPIE 10808, Photonics Applications in Astronomy, Communications, Industry, and High-Energy Physics Experiments 2018, 108082Y, 909 (2018); https://doi.org/10.1117/12.2280983.

[49] K. Tanaka, , *Optical properties and photoinduced changes in amorphous As–S films,* Thin Solid Films, 66, 271 (1980); https://doi.org/10.1016/0040-6090(80)90381-8.

V.M. Kryshenik, A.I. Pogodin, M.J. Filep, I.M. Voynarovych, M.M. Pop, V.V. Rubish, A.V. Gomonnai

В.М. Кришеник[1], А.І. Погодін[2], М.Й. Філеп[2,3], І.М. Войнарович[1], М.М. Поп[2], В.В. Рубіш[1], О.В. Гомоннай[1]

Оптичні властивості стекол As_2S_3:Ag

[1]Інститут Електронної Фізики НАН України, Ужгород, Україна, kryshenik@gmail.com
[2]ДВНЗ «Ужгородський Національний Університет», Ужгород, Україна
[3]Закарпатський угорський інститут ім. Ференца Ракоці ІІ, Берегово, Україна

У статті описано результати вивчення впливу рівня внесення срібла в новосинтезованих стеклах $Ag_x(As_2S_3)_{1-x}$ ($0 \leq x \leq 0.2$) на край оптичного поглинання, ширину забороненої зони і дисперсію показника заломлення у видимому і ближньому інфрачервоному діапазонах. Отримані експериментальні залежності проаналізовано з допомогою одноосциляторної моделі Вемпла–Ді Доменіко. Показано, що зі збільшенням вмісту Ag у склі оптична ширина забороненої зони стає меншою, як і енергія одиночного осцилятора, натомість енергія дисперсії зростає, а ступінь іонності зв'язку залишається практично незмінним.

Ключові слова: аморфні халькогеніди, суперіонні стекла, край оптичного поглинання, показник заломлення.